Evolution of three-dimensional coherent structures in compressible axisymmetric jet

LIU Mingyu (刘明宇), MA Yanwen (马延文) & FU Dexun (傅德薰)

Laboratory of Nonlinear Mechanics, Institute of Mechanics, Chinese Academy of Sciences, Beijing 100080, China
Correspondence should be addressed to LIU Mingyu (email: liumy67@163.com)

Received September 18, 2002

Abstract A high order difference scheme is used to simulate the spatially developing compressible axisymmetric jet. The results show that the Kelvin-Helmholtz instability appears first when the jet loses its stability, and then with development of jet the increase in nonlinear effects leads to the secondary instability and the formation of the streamwise vortices. The evolution of the three-dimensional coherent structure is presented. The computed results verify that in axisymmetric jet the secondary instability and formation of the streamwise vortices are the important physical mechanism of enhancing the flow mixing and transition occurring.

Keywords: jet, vortex ring, streamwise vortex.

DOI: 10.1360/02yw0031

Many important physical characteristics of practical flows, such as the mixing, the flame stability and generation of noise, are related to the mechanism of instability of shear flow, and to the formation and development of the large scale coherent structures. The axisymmetric jet is one of the free shear flows. Study of evolution of three-dimensional coherent structures is very important.

A lot of experimental investigations have been carried out on the axisymmetric jet[1—3]. There have, furthermore, been some numerical simulations on the evolution of three-dimensional coherent structures in jet subject to perturbation in streamwise direction, azimuthal direction and radial direction respectively[3,4], but most of them are incompressible and temporally developing jet. Because of the complex nature of the jet flow, there are many questions to be answered.

In this paper the numerical simulation is used to study the evolution of the three-dimensional coherent structure in the spatially developing compressible axisymmetric jet. The emphasis is on the effects of secondary instability, the formation and the development of streamwise vortex on the enhancing of the flow mixing and transition occurring.

In order to simulate forced "free jet", to study the total effects of the perturbation in streamwise direction, azimuthal direction and radial direction, and to investigate the choice of the most unstable azimuthal mode, a top-hat streamwise velocity profile with random perturbation is used in the jet inlet. This perturbation is of the same amplitude in three directions.

1 Governing equations and discretization

The physical model is shown in fig. 1.

A circular gas flow with a diameter of D spouts into the quiet ambient air and a jet is formed. It is the purpose of this paper to study the three-dimensional evolution of the coherent structure in the spatially developing compressible axisymmetric jet by using direct numerical simulations (DNS).

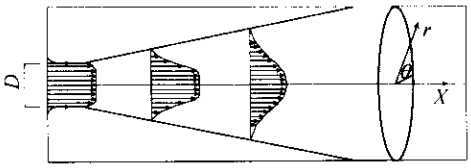

Fig. 1. Schematic diagram of jet flow.

1.1 Governing equations

The three dimensional compressible Navier-Stokes equations in cylindrical coordinates are used to study the development of the axisymmetric jet. To investigate the mixing property of jet and coflow fluid, the passive scalar function f is introduced. It is specified by the following equation:

$$\frac{\partial(rf)}{\partial t}+\frac{\partial(rfu)}{\partial x}+\frac{\partial(rfv)}{\partial r}+\frac{1}{r}\frac{\partial(rfw)}{\partial q}$$
$$=\frac{1}{ReSc}\left[\frac{\partial}{\partial x}\left(m\frac{\partial f}{\partial x}\right)+\frac{\partial}{\partial r}\left(m\frac{\partial f}{\partial r}\right)+\frac{1}{r}\frac{\partial}{\partial q}\left(m\frac{\partial f}{\partial q}\right)+\frac{1}{r}\left(m\frac{\partial f}{\partial r}\right)\right], \tag{1}$$

where Re is the Reynolds number, $Sc=m_0/r_0D_0$ is Schmidt number and D_0 the diffusion efficient of mass, rf denotes the concentration of components per unit volume. In our computing Pr = 1, Sc = 1. At the initial time, f = −1 in the coflow fluid, f = 1 in jet flow and f = 0 at the interface. In the evolution of flow, f > 0 indicates the jet component and f < 0 the coflow component.

1.2 Discretization of differential equations

The fifth order accurate upwind compact difference scheme is used to approximate the convective terms in the N-S equations[5], and the sixth order symmetric compact difference scheme is used to approximate the viscous terms[5], and the three-stage R-K method is used in time direction.

2 Initial condition and boundary condition

In the physical problem to be considered, air jet enters the ambient gas continuously. The entire flow field is statically initialized (u = 0, v = 0, w = 0, r = T =1) at t = 0, the axial velocity profile is specified at the inlet. The boundary condition at the inlet is:

$$f(t,\ 0,\ r,\ q)=\bar{f}+f',\ \text{where } f=r,\ T,\ u,\ v,\ w.$$

Here $\bar{r}$ and $\bar{T}$ are normalized by free incoming conditions, $r'=T'=0$, $\bar{v}=\bar{w}=0$. The axial mean velocity is top-hat profile and properly smoothed by hyperbolic tangent function. It is expressed as

$$\bar{u} = \bar{u}(r) = \begin{cases} 0 & (r > 0.597), \\ \frac{1}{2}[1 - \tanh(a)] & (0.597 \geqslant r \geqslant 0.408), \\ 1 & (r < 0.408), \end{cases} \tag{2}$$

where $a = b(r - 0.5)$, r is the radial coordinate, b is a parameter, $u_i' = e_i(q, t)\bar{u}(r)$, i = 1, 2, 3 correspond to u', v', w' respectively, $e_i(q, t)$ is a computer generated random function and it is changed between (–0.075, 0.075) randomly.

The nonreflecting boundary conditions are applied to the external boundary and outflow boundary of jet flow. The periodic boundary conditions are used in q direction. It should be noted that when the N-S equations in cylindrical coordinates are used, the irregular point will appear at r = 0. In order to avoid this problem, we place the first computation cell at $1/2\Delta r$ away from the centerline. The difference approximation at the points near the centerline, for example the point A at $j = j_0$ in fig. 2, can be obtained by using the values of point B at $j = j_0 + p$. Streamwise velocity (u) is defined by symmetric condition, and radial (v) and azimuthal velocity (w) are defined by anti-symmetric condition. The values of physical parameters at centerline points are the circumferential mean value of adjacent points.

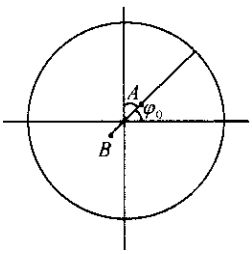

Fig. 2. Schematic diagram of point distribution near the centerline.

3 Computing results and analysis

The higher order accurate method discussed above in this paper is used to simulate the jet flow field. The jet Reynolds number is Re = 15000, Mach number is Ma = 0.6, the computing field is ($12D$, $4.4D$, $2p$) in (x, r, q) directions respectively. The mesh grid number is 151×261×70. The given computing results are all at t = 30.20 if it is not specially noted.

The distribution of passive scalar function f in the plane (0, p), which indicates jet mixing property, is given in fig. 3. This shows the whole topological structure of jet. The computing result

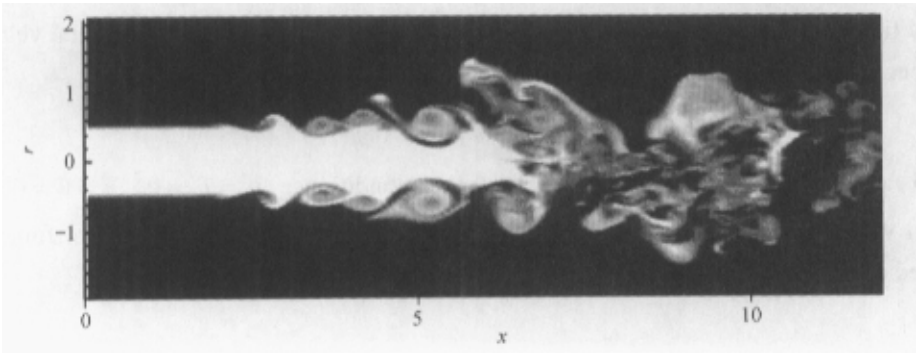

Fig. 3. Distribution of passive scalar on plane (0, p) (t = 30.20).

shows that, in the near field of jet flow, the shear layer formed by the transverse velocity gradient and viscosity effects leads to the K-H instability. The azimuthal perturbation wave is firstly excited (although the same amplitudes of perturbation in streamwise, azimuthal and radial are used at the inlet), so the azimuthal vorticity is redistributed and forms the axisymmetric vortex ring. Fig. 4 shows the azimuthal vorticity field. It can be seen that the regular axisymmetric vertex ring is formed in the flow field at $x \approx 3.0$. The distribution of azimuthal vorticity w_q in cross section at different streamwise location is shown in fig. 5, the axisymmetric vortex ring can also be observed at $x = 2.96$. This result agrees well with the prediction of linear theory[6,7]. From the linear theory we know the most unstable mode is axisymmetric in the initial jet development. Fig. 6 shows the distribution of azimuthal vorticity on 0 plane at different time, which shows the vortex pairing. The formation and development of coherent structures in jet near field are much like the K-H instability of plane mixing layer. There is difference between jet and plane mixing layer. In jet, the axisymmetric vortex ring is formed; the curvature will make vortex ring unstable with its further

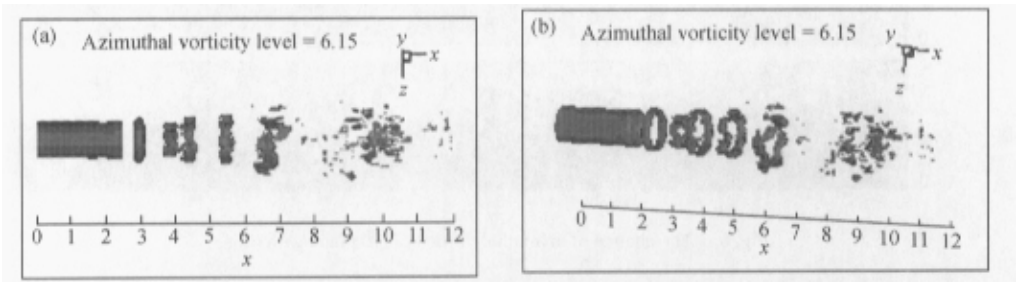

Fig. 4. Distribution of azimuthal vorticity (t =30.20). (a) Perpendicular view; (b) oblique view (30°).

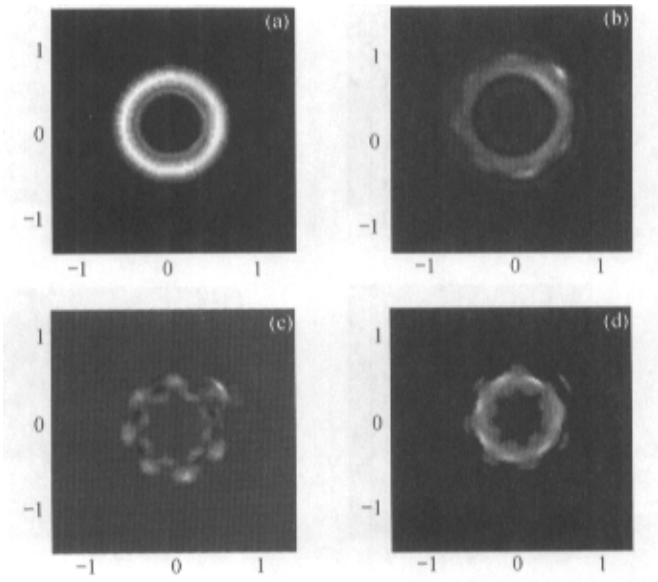

Fig. 5. Distribution of azimuthal vorticity at different streamwise location. (a) x = 2.96 ring zone; (b) x =3.20 braid zone; (c) x =3.44 braid zone; (d) x = 3.68 ring zone.

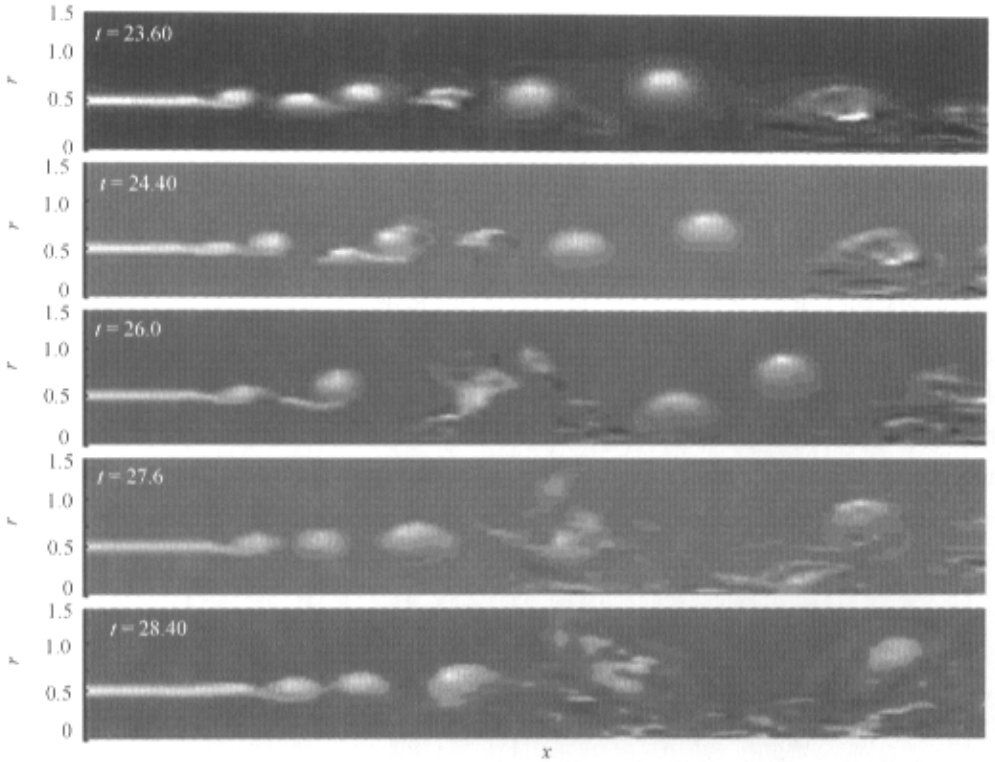

Fig. 6. The change of azimuthal vorticity on 0 plane with time.

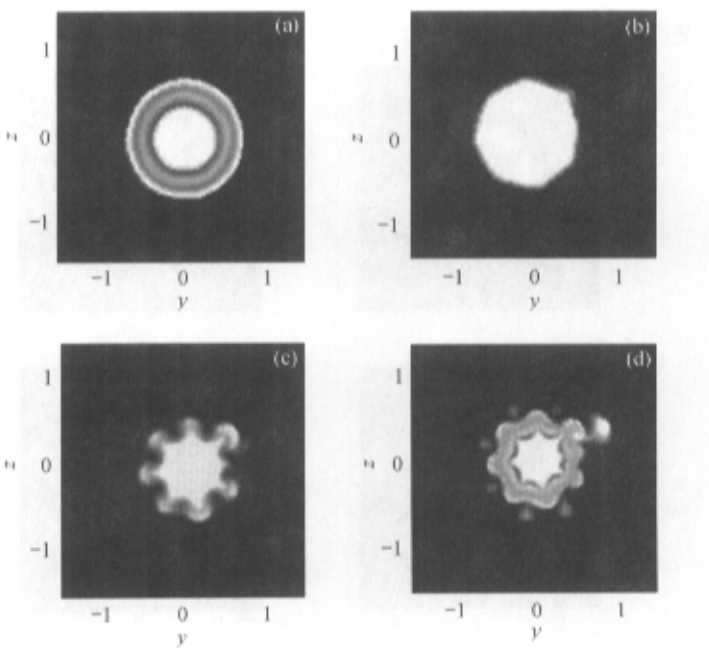

Fig. 7. Distribution of passive scalar at different streamwise location. (a) x = 2.96 ring zone; (b) x =3.20 braid zone; (c) x =3.44 braid zone; (d) x =3.68 ring zone.

development and secondary instability appears; the azimuthal wave breaks its axisymmetry, vortex ring becomes deformed, and three-dimensional structures begin to form. With the natural choice of azimuthal wave number in this paper (random distribution is used in the jet inlet), the vortex ring becomes non-axisymmetric with seven bulges. This can be seen from the distribution of azimuthal vorticity in fig. 5(d) (x = 3.68). Fig. 7 shows the distribution of passive scalar in different cross sections and fig. 7(d) (x = 3.68) shows the same bulges. In fig. 7(c) (x = 3.44), the distribution indicates the formation of mushroom structure, which has been observed in experiments[2]. It still can be seen from fig. 7 that the azimuthal wave breaks its axisymmetric property first in the braid zone (fig. 7(b)). This corresponds to the distribution of azimuthal vorticity in fig. 5(b). The secondary instability leads to the formation and amplification of the streamwise vorticity component. In fig. 8 are given the contours of streamwise vorticity in cross plane at different streamwise location. It can be seen that the amplification of the streamwise vorticity after the sec-

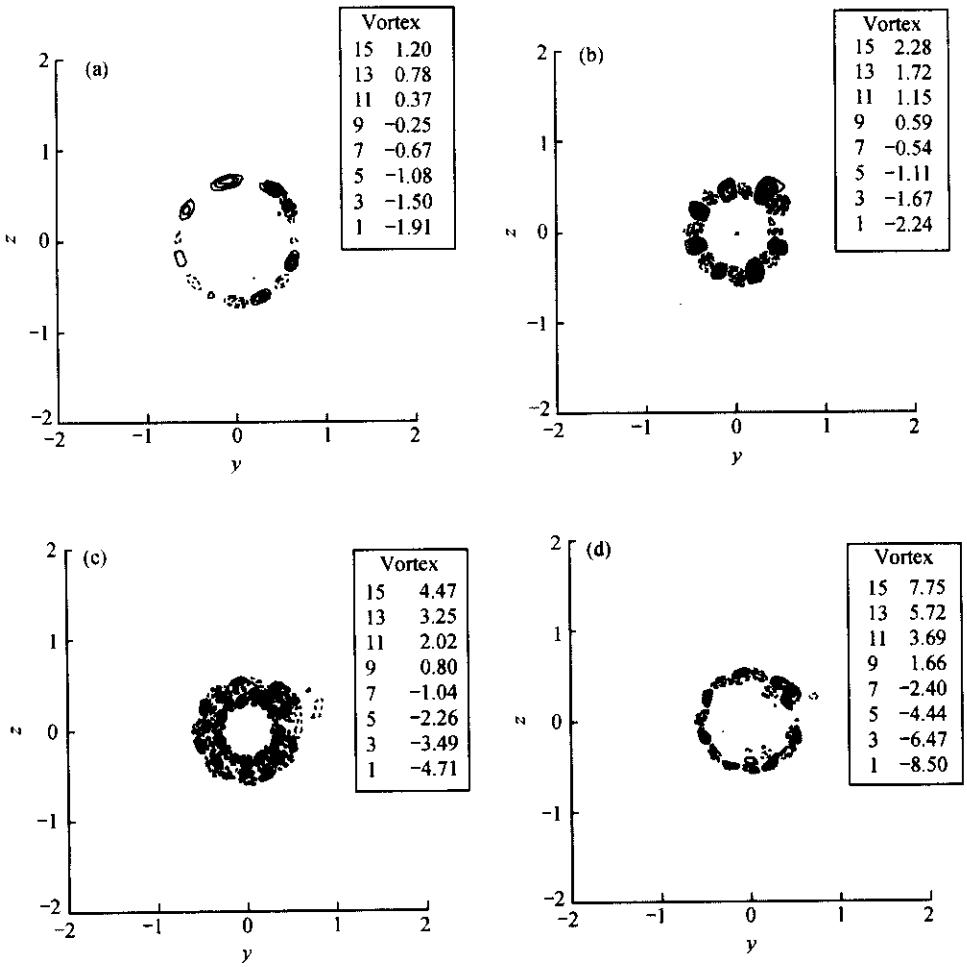

Fig. 8. Contours of streamwise vorticity at different streamwise location. (a) x = 3.20 (braid zone); (b) x = 3.44 (braid zone); (c) x = 3.68 (ring zone); (d) x = 4.08 (braid zone).

ondary instability. At the initial development, the streamwise vorticity has the characteristics of a sheet vortices, whose sign alternates in the circumferential direction (fig. 8(a)); then it is enhanced by the extensional stress induced by the vortex ring and forms counter-rotating streamwise vortex pairs (fig. 8(b)).

In the processes of vortex development, the extensional stress tensor in braid zone induced by the deformation of vortex ring causes the extension and direction change of the streamwise vortex, which forms counter-rotating streamwise vortex pairs. The streamwise vortex wraps with vortex ring, which will augment the streamwise vorticity in the ring zone. This is the coherent structure observed in experiments[2]. Fig. 9 shows the isosurface of streamwise vorticity in flow field (dark color, negative values; light color, positive values). The streamwise vortex pairs for $x > 4.5$ can be seen clearly. The reconnection of vortex ring and the interaction between vortex ring and streamwise vortex lead to formation of double-helix like structure. This structure can also be seen from the isosurface of vorticity in fig. 10, and the three-dimensional structure at $x = 5.5$—9.0 is

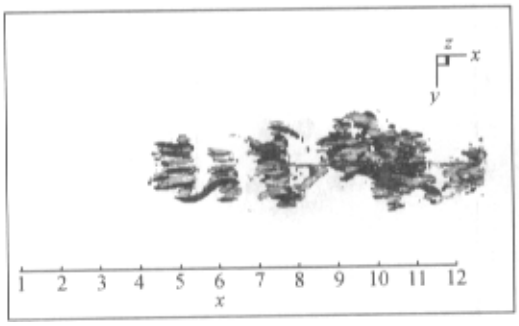

Fig. 9. Isosurface of streamwise vorticity.

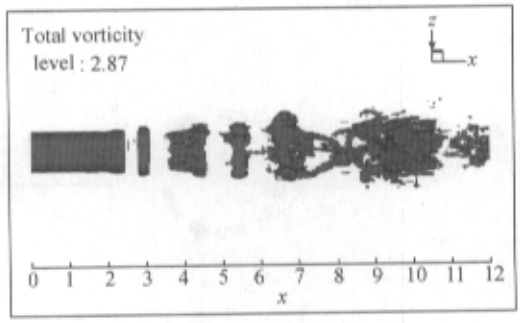

Fig. 10. Isosurface of total vorticity.

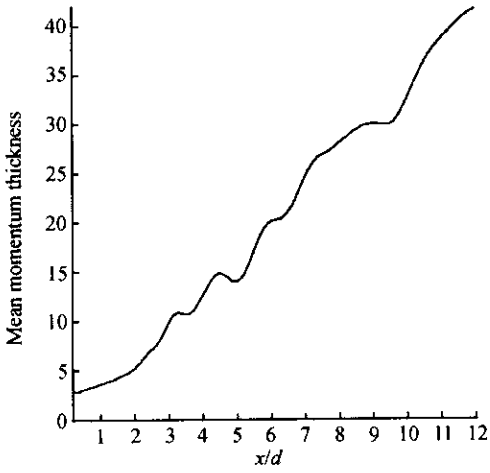

Fig. 11. The variation of jet momentum thickness with streamwise direction.

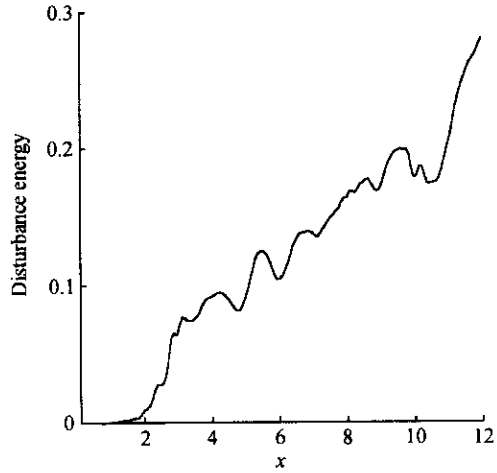

Fig. 12. The variation of jet disturbance energy with streamwise direction.

like that in ref. [8]. The evolution of streamwise vortex enhances the three dimensional perturbation; vortex ring and streamwise vortex break into smaller structures and the flow eventually begins transition and becomes turbulent. The fully developed turbulence has not been reached because of the computing field and mesh grid numbers.

The variation of jet momentum thickness with streamwise direction is given in fig. 11 and disturbance energy in fig. 12. It can be seen that the growth rate of disturbance energy has a large gradient at about $x = 3$, and the momentum thickness has the same appearance. These indicate the secondary instability, the generation of streamwise vortex further exciting the growth of disturbance energy and enhancing the flow mixing. The growth rate of momentum thickness and disturbance energy change abruptly again at about $x = 10$, which indicates the excitation of small scale three-dimensional perturbation. Fig. 13 shows the variation of axial velocity with x. The axial velocity decreases rapidly at about $x = 10$, which also indicates flow begins transition there. The overall flow image in fig. 3 and the distribution of azimuthal vorticity in fig. 4 show clearly the generation of small scale vortex structure.

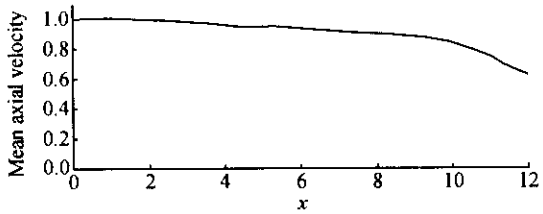

Fig. 13. The variation of jet axial velocity with streamwise direction.

Acknowledgements This work was supported by 973 Program (NKBRSF G 1999032805), and the National Natural Science Foundation of China (Grant Nos. NSAF10176033,10135010).

References

1. Crow, S. C., Champagne, F. H., Orderly structure in jet turbulence, J. Fluid Mech., 1971, 77: 397—413.
2. Liepmann, D., Gharib, M., The role of streamwise vorticity in the near-field entrainment of round jets, J. Fluid Mech., 1992, 245: 643—668.
3. Martin, J. E., Meiburg, E., Numerical investigation of three-dimensionally evolving jets subject to axisymmetric and azimuthal perturbation, J. Fluid Mech., 1991, 230: 271—318.
4. Lienau, J. J., Kollmann, W., Numerical simulation of the turbulent flow in round jets, AIAA, 1993, 93-0547.
5. Fu Dexun, Ma Yanwen, A high order accurate difference scheme for complex flow fields, Journal of Computational Physics, 1997, 134: 1—15.
6. Batchlor, G. K., Gill, A. E., Analysis of the stability of axisymmetric jets, J. Fluid. Mech., 1962, 14: 529.
7. Cohen, J., Wygnanski, I., The evolution of instability in the axisymmetric jet, Part 1, The linear growth of disturbances near the nozzle, J. Fluid Mech., 1987, 176: 191—219.
8. Urbin, G., Calcul par simulation des grandes échelles de la transition turbulente d'un jet libre rond, from Turbulence in Fluids by Marcel Lesieur 1997.